

Effect of impurities on the current magnification in mesoscopic open rings

T. P. Pareek,* P. Singha Deo,[†] and A. M. Jayannavar[‡]

Institute of Physics, Sachivalaya Marg, Bhubaneswar-751005, India

(Received 18 May 1995)

We have considered an open system consisting of a metallic ring coupled to two electron reservoirs. We have recently shown that in the presence of a transport current, circulating currents can flow in such a ring even in the absence of magnetic field. This is related to the current magnification effect in the ring. In our present work we have studied the effect of impurity on the current magnification. We find that the presence of impurity can enhance the current magnification in the loop significantly and thus lead to large circulating currents in a certain range of Fermi energies. This is in contrast to the known fact that impurities can only decrease the persistent currents in closed ring in the presence of magnetic flux.

I. INTRODUCTION

In the past decade physics of mesoscopic systems has emerged as an important area of research from the point of view of basic physics and technology.¹⁻⁴ Mesoscopic physics deals with the structures made of metallic or semiconducting material on a nanometer scale. The length scale associated with the system dimensions in these systems are much smaller than the inelastic mean free path or phase breaking length. In this regime, an electron maintains particle phase coherence across the entire sample. In general, a system with a large degree of freedom is called mesoscopic if the length up to which the wave function retains phase coherence (or, in general, correlation length) exceeds the size of the system. The main characteristics of mesoscopic systems being the quantum coherence. These systems, which are now accessible experimentally, provide an ideal testing ground for our quantum-mechanical models beyond the atomic realm. These systems have revealed, several interesting and previously unexpected quantum effects at low temperatures,¹⁻⁴ which are associated with the quantum interference of electron waves, quantization of energy levels, and discreteness of electronic charge.

A persistent current in small metal rings threaded by magnetic flux is prominent among many quantum effects in submicrometer systems. Büttiker, Imry, and Landauer predicted⁵ the existence of equilibrium persistent currents in an ideal one-dimensional ring in the presence of magnetic flux (ϕ). The magnetic field destroys the time-reversal symmetry and, as a consequence, persistent current (or ring current) flow in the loop and is periodic in magnetic flux, with a period ϕ_0 , ϕ_0 being elementary flux quantum ($\phi_0 = hc/e$). At temperature $T=0$, the amplitude of persistent current is given by ev_f/L , where v_f is the Fermi velocity and L is the circumference of the ring. For spinless electrons persistent current is diamagnetic or paramagnetic for N odd or even, respectively. Several recent experiments⁶⁻⁸ have provided convincing evidence that a normal metal ring threaded by a magnetic flux exhibits in thermodynamic equilibrium a current

that never decays. After these experiments, the persistent current is accepted as a parameter that characterizes equilibrium state of a small metal ring. However, there is a discrepancy up to two orders of magnitude between experimental and theoretical results in the diffusive regime. Attempts to improve upon these results have lead to a spur in the theoretical work on a persistent current in isolated mesoscopic rings. Theoretical studies have been extended to include multichannel rings, and consider the effects of disorder, spin-orbit coupling and electron-electron interaction.⁹⁻¹³ However, the experimental results obtained in the disordered diffusive regime have not yet been explained satisfactorily, despite the intensive theoretical research. The problem of persistent currents has also facilitated the study of some fundamental problems of statistical mechanics, most notably the questions concerning the role of statistical ensemble. The disordered average current is found to be vanishingly small for moderate disorder when grand canonical ensemble is used, whereas it is of finite amplitude within the framework of canonical ensemble.¹

In contrast to the intensity of theoretical studies for isolated systems, the problem of persistent currents in an open system has received less attention.¹⁴⁻²¹ Persistent currents occur not only in isolated rings, but also in the rings connected via leads to electron reservoirs, namely, open systems. A simple open system is shown in Fig. 1,

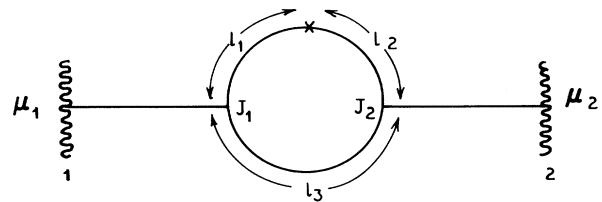


FIG. 1. A metal loop connected to two-electron reservoirs, with chemical potentials μ_1 and μ_2 . There is a δ function potential impurity at the site X in the upper arm.

wherein, the metallic loop is connected to two reservoirs characterized by chemical potentials μ_1 and μ_2 , respectively. Each reservoir acts as a source and sink for electrons and the carriers emerging from the reservoir do not remember their earlier history. The reservoirs absorb carrier energy and thus provides a source of energy dissipation, as well as incoherence. All the scattering processes in the leads including the loop are assumed to be elastic. Inelastic processes occur only in the reservoirs, and hence there is a complete spatial separation between the elastic and the inelastic processes. Weak inelastic processes, however, do not destroy the periodic behavior of persistent currents as a function of magnetic flux ϕ . Open systems provide two distinct possibilities: the first being the equilibrium open system, when $\mu_1 = \mu_2$. The second being the case, $\mu_1 \neq \mu_2$ when a net current flows across the system and this open system corresponds to a nonequilibrium steady state. It is needless to say that equilibrium closed and open systems correspond to different statistical ensemble descriptions, namely, a canonical and a grand canonical ensemble system, respectively. Due to the presence of inelastic scattering (due to reservoirs), the amplitude of persistent currents in equilibrium open system is small as compared to the closed systems.

In our earlier studies, we have pointed out that several effects related to persistent currents can arise in open systems, which have no analog in closed or isolated systems. In particular, we have shown that in the presence of magnetic flux, the magnitude of persistent current is sensitive to the direction of current flow,¹⁸ unlike the physical quantities such as conductance. Also we have discussed the possibility of observing persistent current arising simultaneously due to two nonclassical effects, namely, the Aharonov-Bohm effect and quantum tunneling.¹⁷ In our recent work, we have shown that circulating currents can arise in the presence of a transport current, even in the absence of magnetic field.^{19,20} This is purely a quantum effect and is related to the property of current magnification in the loop. This simple quantum effect can be explained as follows. Consider a system of metallic loop of circumference L coupled to two electron reservoirs, characterized by chemical potentials μ_1 and μ_2 connected via ideal leads as shown in Fig. 1. The leads make the contact with the loop at junction J_1 and J_2 . For simplicity, consider a case without the δ function impurity at X in Fig. 1. The lengths of the upper and lower arms of the loop are $l_1 + l_2$ and l_3 , respectively, such that the length L of the circumference of the loop equals $L = l_1 + l_2 + l_3$. To obtain the transport current, we must have $\mu_1 \neq \mu_2$ (nonequilibrium situation). The transport current will be directed from left to right or from right to left, depending on whether $\mu_1 > \mu_2$ or $\mu_2 > \mu_1$. The current injected¹⁵ by the reservoir into the lead around the small energy interval dE is given by $I_{in} = ev(dn/dE)f(E)dE$, where $v = \hbar k/m$ is the velocity of the carriers at the energy E , $dn/dE = 1/(2\pi\hbar v)$ is the density of states in the perfect wire, and $f(E)$ is the Fermi distribution. The total current flow I in a small energy interval dE through the system is given by the current

injected into the leads by reservoirs multiplied by the transmission probability T . This current splits into I_1 and I_2 in the upper and lower arms such that $I = I_1 + I_2$ (current conservation). As the upper and lower arm lengths are unequal, these two currents are different in magnitude. When one calculates quantum mechanically currents (I_1, I_2) in the two arms, two distinct possibilities exist. The first possibility being for a certain range of incident Fermi wave vectors, the current in the two arms I_1 and I_2 are individually less than the total current I , such that $I = I_1 + I_2$. In such a situation, both currents in the two arms flow in the direction of applied field. However, in certain energy intervals, it turns out that the current in one arm is larger than the total current I (magnification property). This implies that to conserve the total current at the junctions, the current in the other arm must be negative, i.e., the current should flow against the applied external field induced by the difference in the chemical potentials. This is purely a quantum effect. In such a situation, one can interpret that the negative current flowing in one arm continues to flow as a circulating current in the loop.^{19,20} Thus, the magnitude and direction of the circulating current is the same as that of the negative current. Our procedure of assigning a circulating current is exactly the same as the procedure well known in classical *LCR* ac network analysis. When a parallel resonant circuit (capacitance C connected in parallel with a combination of inductance L and resistance R) is driven by external electromotive force (generator), circulating currents arise in the circuit at a resonant frequency.²² This phenomenon is well known as current magnification. For details we refer to Refs. 19, 20, and 22. We would like to emphasize that in our case, for a fixed value of Fermi energy, the circulating current changes sign as we change the direction of the current flow.¹⁹ In equilibrium ($\mu_1 = \mu_2$) we do not obtain any circulating current in the absence of magnetic field. Only in the nonequilibrium situation ($\mu_1 \neq \mu_2$), i.e., in the presence of a steady transport current flow across the system, it is possible to observe the circulating currents.

In this paper, we study the effect of impurity on the current magnification. We have taken the impurity potential to be $V(x) = V\delta(x)$, and the position of impurity is represented by X in the upper arm of the loop. Our motivation to study the impurity effect on current magnification is the following. At a first glance, we naively expect that the presence of impurity leads to increased scattering and hence suppression in the current magnification. However, we show that contrary to expectation, the current magnification can be enhanced in the presence of impurity.

For example, consider a special case of a symmetric loop (both the arms have equal lengths) in the absence of the impurity potential, i.e., $l_1 + l_2 = l_3$, then current magnification is not possible. Because of the symmetry, we shall have $I_1 = I_2 = I/2$ and currents in two arms flowing in the direction of the applied field. Now putting an impurity in one of the arms breaks this symmetry. Thus, in general, $I_1 \neq I_2$ and the current magnification is now possible at particular Fermi energies. So this simple

picture tells us that impurities can enhance the current magnification property. Also, it should be remembered that if we take the extreme limit of $V \rightarrow \infty$, the current in the upper arm is zero ($I_1=0$), and $I_2=I$. In this limit, there can be no circulating current. This simple case suggests that the impurity potential, in general, may help the enhancement of current magnification for particular Fermi energy ranges and also can suppress the amplitude of circulating currents at some other energy ranges. In fact, we show in the following analysis that impurity enhances current magnification drastically for particular values of Fermi energies. The enhanced circulating current at some energies can be as high as 10 000 times the magnitude of the net current flow in the system. In the quantum case discussed here, there is no principle restricting the upper bound of current magnification and it can be arbitrarily large without violating the basic law of conservation of the current at the junctions (Kirchoff's law). In a closed isolated loop, in the presence of magnetic flux ϕ , a persistent current carried in by single-particle energy level ϵ_n is given by $I_n = -\partial\epsilon_n/\partial\phi$, and the total current is $I = \sum I_n f(\epsilon_n)$, where $f(\epsilon_n)$ is the Fermi function. In this case, the presence of impurity in the otherwise ideal loop leads to scattering, which lifts the degeneracy of states (level repulsion) at the values $\phi=0, \pm\phi_0/2, \dots$ etc. (at Brillouin-zone boundaries). This in turn flattens the energy curve as a function of ϕ and as a result the ampli-

tude of persistent current always decreases with an increase in the impurity strength (for details see Ref. 9).

II. THEORETICAL TREATMENT

We now consider a case of one-dimensional metal loop of length L coupled to two-electron reservoirs, as shown in Fig. 1, and a current is injected into the metal loop from the left ($\mu_1 > \mu_2$). Our calculation is for a noninteracting system of electrons. Except at the δ potential impurity (of strength V) at site X , the potential throughout the network is zero (free electron network). We do not assume any particular form for the scattering matrix for the junctions J_1 and J_2 , but scattering at the junctions follow from the first principles using quantum mechanics. At temperature zero, the total current flow around a small energy interval dE around E is $I = (e/2\pi\hbar)TdE$, where T is the transmission coefficient calculated at the energy E . It is a straight forward exercise to set up a scattering problem and calculate the transmission coefficient (T) and the current densities in the upper (I_1) and the lower (I_2) arms. We follow our earlier method of quantum waveguide transport on networks closely to calculate these quantities.^{17-20,23-25} We have imposed the Griffiths boundary condition (conservation of current) and single valuedness of the wave functions at the junctions. The final analytical expressions for the current densities are given by

$$\frac{dI}{dE} = (e/2\pi\hbar)T, \quad (1)$$

$$\begin{aligned} T = & 16\{V^2\cos^2[k(l_1-l_2)] - 2V^2\cos[k(l_1-l_2)]\cos[k(l_1+l_2)] \\ & + V^2\cos^2[k(l_1+l_2)] + 4kV\cos[k(l_1-l_2)]\sin[k(l_1+l_2)] - 4kV\cos[k(l_1+l_2)]\sin[k(l_1+l_2)] \\ & + 4k^2\sin^2[k(l_1+l_2)] + 4kV\cos[k(l_1-l_2)]\sin[kl_3] - 4kV\cos[k(l_1+l_2)]\sin[kl_3] \\ & + 8k^2\sin[k(l_1+l_2)]\sin[kl_3] + 4k^2\sin^2[kl_3]\} / \Omega, \end{aligned} \quad (2)$$

$$\begin{aligned} \frac{dI_1}{dE} = & (e/2\pi\hbar)16k\{2k - 2k\cos(2kl_3) + 2k\cos(kr) - 2k\cos(kL) \\ & - V\sin(kp) + V\sin(kr) + V\sin(ks) - V\sin(kL)\} / \Omega, \end{aligned} \quad (3)$$

$$\begin{aligned} \frac{dI_2}{dE} = & -(e/2\pi\hbar)16\{-2k^2 - V^2 + V^2\cos[2kl_1] - V^2\cos[2kl_1]\cos[2kl_2] + V^2\cos[2kl_2] \\ & + 2k^2\cos[2k(l_1+l_2)] - 2k^2\cos[kr] + 2k^2\cos[kL] - 2kV\sin[2kl_1] - 2kV\sin[2kl_2] \\ & + 2kV\sin[2k(l_1+l_2)] + kV\sin[kp] - kV\sin[kr] - kV\sin[ks] + kV\sin[kL]\} / \Omega, \end{aligned} \quad (4)$$

where

$$\begin{aligned}
\Omega = & \{ 64k^2 + 4V^2\cos^2[kp] + 32k^2\cos[kr] + 4k^2\cos^2[kr] + 32V^2\cos[kp]\cos[ks] \\
& + 4V^2\cos^2[ks] - 160k^2\cos[kL] - 16V^2\cos[kp]\cos[kL] \\
& - 40k^2\cos[kr]\cos[kL] - 16V^2\cos[ks]\cos[kL] + 100k^2\cos^2[kL] \\
& + 16V^2\cos^2[kL] - 16kV\sin[kp] - 4kV\cos[kr]\sin[kp] + 20kV\cos[kL]\sin[kp] + V^2\sin^2[kp] + 16kV\sin[kr] \\
& + 4kV\cos[kr]\sin[kr] - 20kV\cos[kL]\sin[kr] - 2V^2\sin[kp]\sin[kr] \\
& + V^2\sin^2[kr] + 16kV\sin[ks] + 4kV\cos[kr]\sin[ks] \\
& - 20kV\cos[kL]\sin[ks] - 2V^2\sin[kp]\sin[ks] + 2V^2\sin[kr]\sin[ks] + V^2\sin^2[ks] - 80kV\sin[kL] \\
& + 32kV\cos[kp]\sin[kL] - 20kV\cos[kr]\sin[kL] + 32kV\cos[ks]\sin[kL] + 36kV\cos[kL]\sin[kL] \\
& + 10V^2\sin[kp]\sin[kL] - 10V^2\sin[kr]\sin[kL] - 10V^2\sin[ks]\sin[kL] + 64k^2\sin^2[kL] + 25V^2\sin^2[kL] \} . \quad (5)
\end{aligned}$$

In the above equations, $k = \sqrt{E}$ is the incident wave vector, $p = l_1 - l_2 - l_3$, $L = l_1 + l_2 + l_3$, $r = l_1 + l_2 - l_3$, and $s = l_1 - l_2 + l_3$. We have rescaled current densities in a dimensionless form and henceforth, we denote $I(\equiv 2\pi\hbar/e dI/dE)$, $I_1(\equiv 2\pi\hbar/e dI_1/dE)$, and $I_2(\equiv 2\pi\hbar/e dI_2/dE)$ and we have set units of \hbar and $2m$ to be unity.

III. RESULTS AND DISCUSSIONS

In the limit $V=0$, our expressions agree with earlier known results.^{19,20} We have studied the behavior of I_1 and I_2 , as a function of Fermi wave vectors and identify the wave-vector intervals, wherein either the I_1 or I_2 flows in the negative direction for $V \neq 0$. In any range of Fermi energy if one of them (I_1 or I_2) is negative, then the magnitude of the negative current gives the circulating current. When I_1 is negative, the direction of circulating current is anticlockwise and when I_2 is negative, then it is clockwise. A clockwise circulating current is taken to be positive and an anticlockwise as negative according to the usual convention followed for persistent currents in closed rings. Having defined a circulating current in this manner, we plot in Fig. 2 a circulating current versus kL for two values of the impurity potential strength. The solid curve is for $VL=0$ and the dotted curve is for $VL=1$. In both the cases, we take $l_1/L=0.3125$, $l_2/L=0.3125$, and $l_3/L=0.375$. The figure shows that the dotted curve is slightly shifted towards a higher energy axis, with respect to the solid curve and the first peak value of it is larger than that of the solid curve. It shows that in the first energy range where we obtain a circulating current, the amplitude of the current is actually enhanced by the impurity potential and the position of this range of Fermi energy is modified due to the impurity. The amplitude of the first negative peak in the circulating current decreases, and the circulating current behavior in the interval of kL between 10–15 is qualitatively modified. As discussed in our earlier paper,¹⁹ the nature of the circulating current depends on the zero-pole pair structure in the transmission amplitude. The circulating current arises near the poles (or at a real value of the pole in the complex plane) in the

transmission amplitude. An imaginary value of the poles in the complex plane determines the width of the peak. The poles determine the resonant states of the system. The smaller the imaginary value is the narrower the peak is. The shift in the peak position on the real axis is attributed to the fact that the position of the poles change as we change the impurity potential. The circulating current is also enhanced at some other Fermi energy ranges, whereas at some others it is suppressed, because of the impurity. This happens because of the fact that circulating current, due to current magnification, has a completely different origin than that of persistent currents due to the presence of magnetic field in closed isolated rings.

Several circulating current peaks exhibit exotic behavior, as we keep increasing the impurity strength. For the sake of clarity, we will consider only the behavior

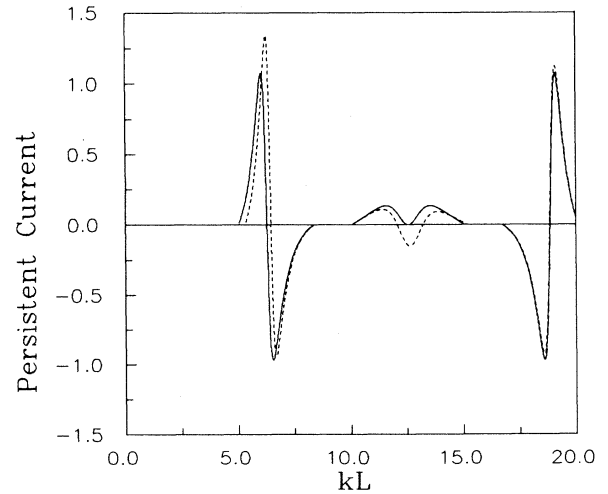


FIG. 2. Plot of circulating current versus kL for $VL=0$ (solid line) and $VL=1$ (dotted line). In both the cases $l_1/L=0.3125$, $l_2/L=0.3125$, and $l_3/L=0.375$.

of circulating currents in the first range of kL around which circulating current arises. In Fig. 3, we plot circulating current versus kL for various values of VL in the first energy range, which keeps changing with change in VL . The curves a , b , c , d , and e are for $VL=5, 10, 15, 20$, and 25 , respectively. For all the curves, we take $l_1/L=0.3125$, $l_2/L=0.3125$, and $l_3/L=0.375$. The figure shows that initially the magnitude of the first peak on the positive side increases monotonously and also the peak position shifts towards higher energy with VL . However, as the magnitude of the peak value at the maximum increases, the width of the peak decreases. On the other hand, the magnitude of the circulating current peak on the negative side in this first energy range is not so sensitive to the impurity strength VL . Initially, as VL increases, it decreases slightly. This can be seen by observing the curves a , b , c , and d . For curve e this peak on the negative side has increased slightly with respect to the curve d . So this negative side peak exhibits a small oscillatory behavior with VL . However, the width of this negative peak monotonously decreases as a function of the strength of the impurity in the given range of potential strength considered in the figure. Needless to say that the shape of the peaks also reflects the nature of density of states around the position of the peak (or at resonance). Enhancement of density of states around the poles leads to large circulating currents. This can be easily verified by calculating the density of states near the poles by using Friedel's theorem,²⁶ according to which change in density of states due to a scatterer, at a particular energy is given by $1/\pi d\theta/dE$, where θ is the argument of the complex transmission amplitude.

From now on we study the behavior of the maximum value (I_{\max}) of the first circulating current peak on the positive side as a function of the impurity strength. The position of the I_{\max} on the real kL axis is given by the real part of the pole in the transmission amplitude (or scattering amplitude) in a complex kL plane. It is clear from the earlier Fig. 3 that I_{\max} increases initially as a function of VL . In Fig. 4, we have plotted I_{\max} versus VL , the values of the physical parameters l_1/L , l_2/L , and l_3/L are the same as that used for Fig. 3. We numerically evaluate I_{\max} of the circulating current (at the first peak) for a fixed value of VL and then slowly change VL up to $VL=31$ in order to plot the peak value at the maximum of circulating current versus VL . In Fig. 4, we have not shown the behavior of I_{\max} in the range $VL=(28.0)$ to $VL=(29.1)$ as the magnitude of the I_{\max} increases rapidly and goes beyond the scale. Between a value of $VL=28$ and $VL=29$, the I_{\max} is several orders of magnitude larger than the total current I through the sample and the corresponding widths of the peaks are extremely small. For example $I_{\max}=111.123, 175.687, 709.423, 8958.1428$, and 11755 for values of $VL=28.2, 28.5, 28.9, 28.99$, and 29.01 , respectively, and the peak value I_{\max} on kL axis corresponds to $kL=8.3549242, 8.3633125, 8.374304, 8.37674705$, and 8.377288471 , respectively. In fact, I_{\max} diverges for $VL=(29)$ (for this case, corresponding $kL=8.37701785204$). Above $VL=29$, the I_{\max} shows a drastic fall in the magnitude

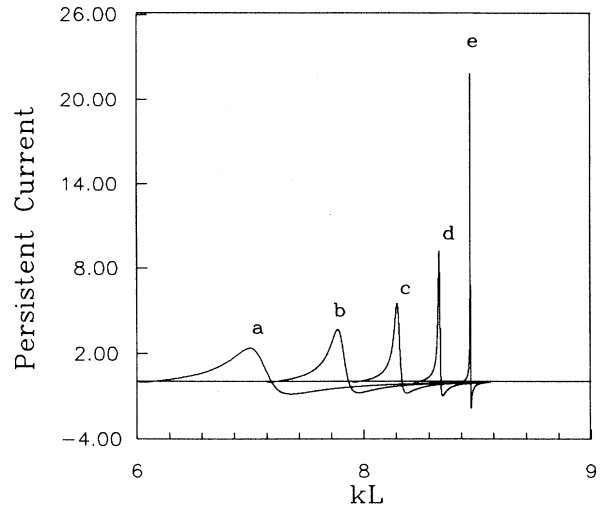


FIG. 3. Plot of circulating current versus kL for various value of VL in the first energy range. The curves a , b , c , d , and e are for $VL=5, 10, 15, 20$, and 25 , respectively. For all the curves $l_1/L=0.3125$, $l_2/L=0.3125$, and $l_3/L=0.375$.

and as expected it reaches the value zero in the limit $VL \rightarrow \infty$. In this limit, the current in the upper arm is zero ($I_1=0$) and $I_2=I$ and hence no circulating current flows. Our above observations clearly indicate that there is no upper bound for the current magnification (same as in the case for classical LCR networks driven by external ac electromotive force²² in the limit the magnitude of resistance $R \rightarrow 0$). For the particular case considered here, as we increase impurity strength initially it helps the current magnification and on reaching a critical value (at which current magnification diverges) a further in-

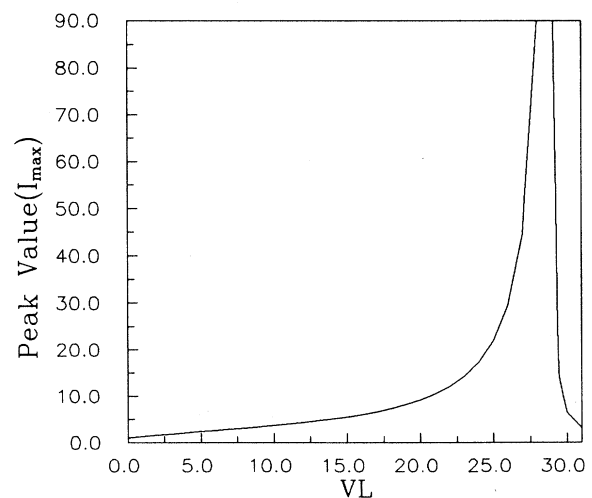


FIG. 4. The figure shows the scaling of I_{\max} with VL for $l_1/L=0.3125$, $l_2/L=0.3125$, and $l_3/L=0.375$.

crease in the impurity strength decreases the current magnification. Thus impurity, in general, can play a dual role of enhancing, as well as suppressing the current magnification effect.

To analyze in some details the divergence in current magnification, we study the imaginary part of the pole $I_m(p)$ in the complex kL plane. In Fig. 5, we have plotted the imaginary part of the pole (first pole) corresponding to Fig. 4 (by analyzing the transmission amplitude in the complex kL plane), as a function of VL . All the physical parameters are the same as that used for Fig. 4. One can immediately notice that the imaginary part of the pole decreases as we increase VL . This corresponds to a situation where the current magnification increases as a function of VL . At a value of $VL=(29)$, an imaginary part approaches zero. This is the same value of VL , where the current magnification exhibits divergence. In a sense, the divergence of current magnification occurs as poles of a transmission amplitude in the complex plane approaches the real axis. The lifetime of the resonant state (corresponding to poles) is inversely proportional to the imaginary part of the pole. The imaginary part being zero implies that the resonant state has an infinite lifetime, and hence is a bound state. This bound state is localized across the loop and corresponds to a von Neumann and Wigner-type bound state in continuum.^{24,27} As we increase VL further, the imaginary part increases and consequently the peak value of circulating current decreases.

The circulating current due to current magnification generally appears around the zeros of the transmission coefficient, but there can be cases where this is not true, as shown in Fig. 6. Here, we have plotted circulating current (solid curve) and the transmission coefficient (dashed curve) versus kL for $VL=20$, $l_1/L=0.3125$, $l_2/L=0.3125$, and $l_3/L=0.375$. In the kL range from 34 to 45, we find a large circulating current and around this region T goes to zero nowhere, but has a minimum (antiresonance). As mentioned in the Introduction, in the special case of a metal loop with two equal arms and without the presence of impurity, the currents I_1 and I_2

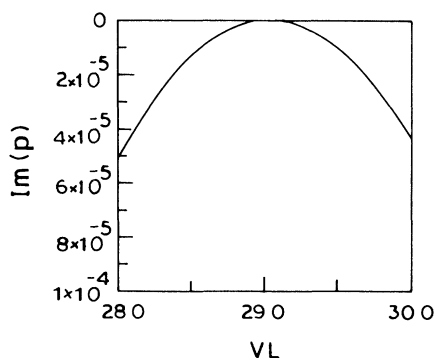


FIG. 5. The plot of the strength or magnitude of the imaginary part of the first complex pole of the transmission amplitude versus VL for $l_1/L=0.3125$, $l_2/L=0.3125$, and $l_3/L=0.375$.

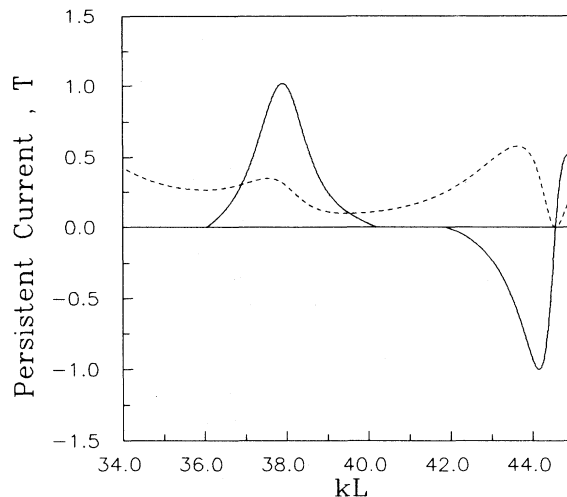


FIG. 6. Plot of the circulating current (solid curve) and transmission coefficient (dashed curve) versus kL for $VL=20$, $l_1/L=0.3125$, $l_2/L=0.3125$, and $l_3/L=0.375$.

on the arms (due to symmetry reasons) are equal and each equal half of I at all Fermi energies. So at no Fermi energy interval we get a circulating current according to our definition for it as stated earlier. However, a small impurity in one of the arms breaks the above symmetry and the currents I_1 and I_2 are not equal. This gives rise to the circulating current in a certain range of the Fermi energies, and we find that as the impurity strength is increased from zero, initially the circulating current amplitudes in all the relevant kL intervals show a tendency to increase.

So far we have discussed the effect of the impurity strength on the current magnification. In the following, we consider the effect of the impurity position on the current magnification. For this we consider a fixed impurity strength and fixed upper and lower arm lengths. In Fig. 7, we have plotted the circulating currents as a function of kL for a fixed value of impurity strength $VL=(10)$ and the impurity placed at various different positions in the upper arm. The solid curve is the case when the impurity is placed in the middle of the upper arm ($l_1/L=0.3125$, $l_2/L=0.3125$, and $l_3/L=0.375$), whereas the dashed curve is for the impurity position away from the center of the arm ($l_1/L=0.4$, $l_2/L=0.225$, and $l_3/L=0.375$). We observe drastic changes in the nature, height, and width of the circulating current peaks in the two cases. Again, this can be explained from the point of view of the shift in the pole structure for the two different cases.

In conclusion, we have studied the effect of impurity on the current magnification in an open metallic loop in the presence of a transport current. In this nonequilibrium a steady-state circulating current arises even in the absence of magnetic field. More importantly, we have shown that the presence of impurity can dramatically enhance the current magnification effect at particular values of Fermi energies, whereas it can decrease the

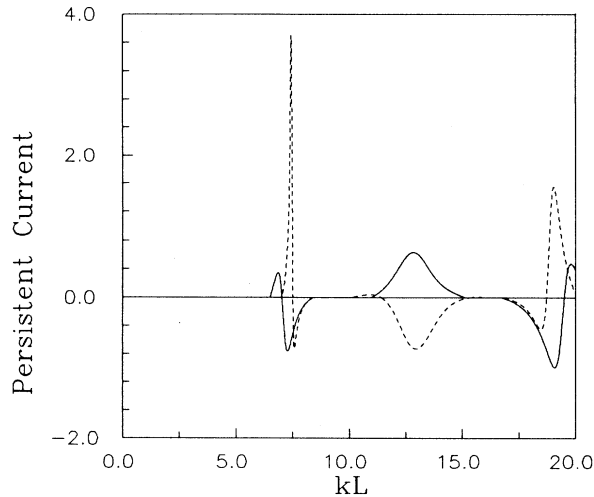


FIG. 7. Plot of circulating current versus kL for $VL=(10)$ and for two positions, respectively, of the impurity in the upper arm. The solid curve is for $l_1/L=0.3125$, $l_2/L=0.3125$, and $l_3/L=0.375$. The dotted curve is for $l_1/L=0.4$, $l_2/L=0.225$, and $l_3/L=0.375$.

current magnification at some other values of Fermi energies. We have shown that current magnification property is not only sensitive to the impurity strength, but also sensitive to its position. This is in contrast to the effect of the presence impurity on persistent currents in closed isolated metallic rings, where persistent currents are always

suppressed as one increases the impurity strength. Since the underlying principle of circulating currents in open systems in the presence of a transport current (and in the absence of magnetic field) is different from the persistent currents in isolated rings in the presence of magnetic flux, we expect that even in the presence of random impurities, one should expect current magnification of observable magnitudes in open systems in the presence of a transport current. Work along these lines is in progress. The circulating current changes sign if we change the direction of the current and hence at equilibrium ($\mu_1=\mu_2$) no circulating currents are possible. Since the magnetic moment of the loop is proportional to the line integral of the current (i.e., the total current integrated over Fermi energies between μ_1 and μ_2 at temperature $T=0$) along the entire circumference of the loop, due to the current magnification effect, we expect that one should observe enhanced magnetic response around particular Fermi energy intervals. This can be achieved experimentally by having a gate (which mimics the impurity potential) in one of the arms and by appropriately tuning the gate voltage and Fermi energy or ($\mu_1-\mu_2$). The experiment will show dramatic enhancement in the magnetic response. The effect of the magnetic field on the current magnification will be presented in future studies.

ACKNOWLEDGMENTS

One of us (A.M.J.) thanks Professor A. G. Aronov and Professor V. E. Kravtsov for several useful discussions during the initial stages of this work and Professor N. Kumar for continued discussions on this subject.

*Electronic address: pareek@iopb.ernet.in

†Electronic address: prosen@iopb.ernet.in

‡Electronic address: jayan@iopb.ernet.in

¹Quantum Coherence in Mesoscopic Systems, Vol. 254 of NATO Advanced Study Institute Series B: Physics, edited by B. Kramer (Plenum, New York, 1991).

²Science and Engineering of One and Zero Dimensional Semiconductors, Vol. B 214 of NATO Advanced Study Institute, Series B: Physics, edited by S. P. Beaumont and C. M. Sotomayor Torres (Plenum, New York, 1990).

³Transport Phenomena in Mesoscopic Systems, edited by H. Fukuyama and T. Ando (Springer-Verlag, Berlin, 1992).

⁴S. Washburn and R. A. Webb, Adv. Phys. **35**, 75 (1986).

⁵M. Büttiker, Y. Imry, and R. Landauer, Phys. Lett. **96A**, 365 (1983).

⁶L. P. Levy, G. Dolan, J. Dunsmuir, and H. Bouchiat, Phys. Rev. Lett. **64**, 2074 (1990).

⁷V. Chandrasekhar, R. A. Webb, M. J. Brady, M. B. Ketchen, W. J. Gallagher, and A. Kleinsasser, Phys. Rev. Lett. **67**, 3578 (1991).

⁸D. Mailly, C. Chapelier, and A. Benoit, Phys. Rev. Lett. **70**, 2020 (1993).

⁹H. F. Chung, Y. Gefen, E. K. Riedel, and W. H. Shih, Phys. Rev. B **37**, 6050 (1988).

¹⁰H. F. Chung and E. K. Riedel, Phys. Rev. B **40**, 9498 (1989).

¹¹G. Montambaux, H. Bouchiat, D. Sigei, and R. Freisner, Phys. Rev. B **42**, 7647 (1990).

¹²O. Entin-Wohlman, Y. Gefen, Y. Meier, and Y. Oreg, Phys.

Rev. B **45**, 11 890 (1992).

¹³P. Kopeitz, Int. J. Mod. Phys. B **8**, 2593 (1994), and references therein.

¹⁴M. Büttiker, Phys. Rev. B **32**, 1846 (1985).

¹⁵M. Büttiker, in SQUIDS '85-Superconducting Quantum Interference Devices and their Applications (de Gruyter, Berlin, 1985), p. 529.

¹⁶P. A. Mello, Phys. Rev. B **47**, 16 358 (1993).

¹⁷P. Singha Deo and A. M. Jayannavar, Mod. Phys. Lett. B **7**, 1045 (1993).

¹⁸P. Singha Deo and A. M. Jayannavar, Phys. Rev. B **49**, 13 685 (1994).

¹⁹A. M. Jayannavar and P. Singha Deo, Phys. Rev. B **51**, 10 175 (1995).

²⁰A. M. Jayannavar, P. Singha Deo, and T. P. Pareek, in Proceedings of International Workshop on Novel Physics in Low-Dimensional Electron Systems, Madras, India [Physica B **212**, 216 (1995)].

²¹D. Takai and K. Ohta, Phys. Rev. B **48**, 14 318 (1993).

²²D. F. Shaw, An Introduction to Electronics, 2nd ed. (Longman, London, 1970), p. 51.

²³A. M. Jayannavar and P. Singha Deo, Mod. Phys. Lett. B **8**, 301 (1994).

²⁴P. Singha Deo and A. M. Jayannavar, Phys. Rev. B **50**, 11 629 (1994).

²⁵J. Xia, Phys. Rev. B **45**, 3593 (1992).

²⁶J. Friedel, Adv. Phys. **3**, 466 (1954).

²⁷J. von Neumann and E. Wigner, Z. Phys. **30**, 4635 (1929).